Photophysical and Phototoxic Properties of the Antibacterial Fluoroquinolones Levofloxacin and Moxifloxacin

by **Giampietro Viola***[a]), **Laura Facciolo**[a]), **Marcella Canton**[b]), **Daniela Vedaldi**[a]), **Francesco Dall'Acqua**[a]), **Gian Gaetano Aloisi**[c]), **Matteo Amelia**[c]), **Arianna Barbafina**[c]), **Fausto Elisei**[c]), and **Loredana Latterini**[c])

[a]) Department of Pharmaceutical Sciences, University of Padova, via Marzolo 5, I-35131 Padova (fax: 049 8275366; e-mail: giampietro.viola.1@unipd.it)

[b]) Dipartimento di Chimica Biologica, Università di Padova, I-35131 Padova

[c]) Dipartimento di Chimica, Università di Perugia, I-06123 Perugia

Two antibacterial fluoroquinolones, levofloxacin and moxifloxacin, were investigated to evaluate their photophysical properties and to explore the mechanism of their phototoxicity. Photophysical experiments were carried out in aqueous solution by stationary and time-resolved fluorimetry, and by laser flash photolysis, to obtain information on the various decay pathways of the excited states of the drugs and on transient species formed upon irradiation. The results obtained show that levofloxacin is able to photosensitize red blood cell lysis in an oxygen-independent way and induce a high decrease in cell viability after UVA irradiation, although to a lesser degree than the racemic mixture ofloxacin. Moxifloxacin, which is an 8-MeO-substituted fluoroquinolone, is less phototoxic than the other compounds. Cellular phototoxicity was inhibited by the addition of superoxide dismutase, catalase, and free radical and hydroxyl radical scavengers (BHA, GSH, mannitol, and DMTU), indicating the involvement of superoxide anion and/or a radical mechanism in their cytotoxicity. A good correlation was observed between lipid peroxidation, protein photodamage, and cellular phototoxicity, indicating that test compounds exert their toxic effects mainly in the cellular membrane. Experiments carried out on pBR322 DNA show that these derivatives do not significantly photocleave DNA directly, but single-strand breaks were evidenced after treatment of photosensitized DNA by two base-excision-repair enzymes, and Endo III.

Introduction[1]). – The fluoroquinolones are an important class of antimicrobials whose potential clinical usefulness continues to expand [1]. Quinolones are potent chemotherapeutic agents of first choice for the treatment of a broad range of bacterial infections, and their toxicity is low and comparable to that of other commonly used antimicrobial agents; thus quinolones can be considered to be relatively well-tolerated [2][3]. However, they occasionally produce side effects such as acute dermatitis, which

[1]) *Abbreviations:* ΔA, change of absorbance; B, benzophenone, BER, base-excision-repair enzymes; BHA, '2,6-di-(*tert*-butyl)hydroxyanisole' (=2,6-bis(1,1-dimethylethyl)-4-methoxyphenol); BSA, bovine serum albumin; CAT, catalase; Endo III Endonuclease III; Fpg, Formammido pyrimid glycosilase; DMTU, *N*,*N*′-dimethylthiourea; F, fluorescence; FCCP, {[4-(trifluoromethoxy)phenyl]hydrazono}propanedinitrile; GSH, glutathione reduced form; ISC, intersystem crossing; k, monomolecular decay-rate parameter; k_{ox}, bimolecular rate parameter for triplet quenching by molecular oxygen; LVX, levofloxacin, MAN, mannitol; MOX moxifloxacin; MTT, 3-(4,5-dimethylthiazol-2-yl)-2,5-diphenyltetrazolium bromide; PI, photoionization; RBC, red blood cells; S, singlet; ROS, reactive oxygen species; SOD, superoxide dismutase; T, triplet; TBA, thiobarbituric acid; TBARS, thiobarbituric acid reactive substances; TMRM, tetramethylrhodamine methyl ester; TFE, 2,2,2-trifluoroethanol; ε, molar absorption coefficient; λ_{exc}, excitation wavelength; λ_{max}, maximum absorption wavelength; τ, lifetime; ϕ, quantum yield; $\Delta\psi_m$, mitochondrial membrane potential.

are usually confined to areas of the skin exposed to sunlight. The phototoxic mechanism(s) as the cause of abnormal photosensitivity and its relationship to chemical structure remain unclarified.

Many studies on the phototoxic properties of these drugs have been reported in the last decades, and structure–side-effects relationships of newly developed fluoroquinolones have been evaluated [2]. Primary acute and chronic lesions involving the photosensitized skin are erythema, edema, and pruritus, and, in more-severe cases, blistering and vesicles of the exposed parts [4]. These kind of skin alterations may deteriorate into cancer [5].

The action of these photosensitizers is dependent on the production of extremely reactive molecules (reactive oxygen species, free radicals, photoproducts), which are able to modify the cell components, including lipids, proteins, and nucleic acids, in combination with UVA; it has been suggested that the most-phototoxic quinolones are those that induce the formation of reactive oxygen species (ROS), because these species cause severe tissue damage [6–8]. However, a correlation between the production of ROS and the phototoxic potency of fluoroquinolones cannot be drawn, and other mechanisms, *i.e.*, generation of highly reactive photodegradation products, seem to be involved [9].

Levofloxacin (LVX) and moxifloxacin (MOX) are two new compounds recently introduced in therapy. The former is the (*S*)-isomer of ofloxacin, which is reported to have antimicrobial activity twice as high as the racemic mixture ofloxacin, against a variety of *Gram*-positive and *Gram*-negative bacteria [10–12]. MOX is a fluoroquinolone in which the position 7 of the fluoroquinolone ring is substituted by an octahydropyrrolo[3,4-b]pyridine moiety, and its position 8 is modified with a MeO group. The present paper presents a photophysical and photobiological investigation of these fluoroquinolones. The purpose is to obtain a complete and comparative picture of the photosensitizing effects of these drugs on the main cellular targets, including a description of the action mechanism and the involved species. In particular, the studies on fluoroquinolones in aqueous solutions were based on a characterization of lowest singlet and triplet states by stationary and pulsed fluorimetry, and by laser flash photolysis. The transient species formed by laser excitation were characterized in terms of spectra, and decay times and their reactivity against model biological molecules were investigated.

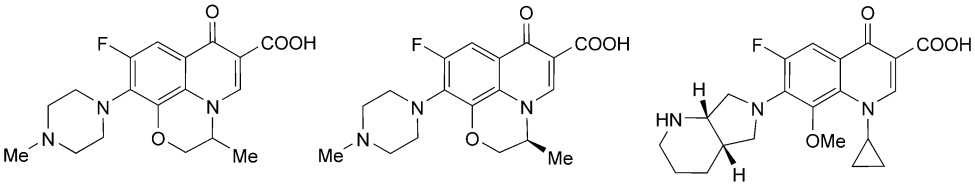

The phototoxic potential of fluoroquinolones was investigated by several *in vitro* techniques, including analysis of erythrocytes lysis and cytotoxicity in mammalian cells. The study was extended by investigating the phototoxic effects of the drugs on

biological substrates such as lipids, proteins, and DNA. This approach represents an useful tool for elucidating the mechanism(s) by which these fluoroquinolones induce skin photosensitization, and it can be useful for further studies on the prediction of the phototoxicity of other correlated compounds.

Results and Discussion. – The absorption spectra of fluoroquinolones MOX and LVX in MeCN and aqueous solutions at different pH values are shown in *Fig. 1*. Both compounds in the UV/VIS region exhibit two absorption bands whose positions are affected by the solvent polarity/proticity. In particular, in H_2O the main band is centered around 290 nm and the second one at 330–335 nm. In MeCN, the spectra are red-shifted, and a shoulder appears in the red-edge of the spectrum (*ca.* 360 nm), indicating that, in this less polar and non-protic solvent, the lowest singlet excited state is stabilized. The main bands have molar absorption coefficients in the order of $1-3\times 10^4\ \text{M}^{-1}\,\text{cm}^{-1}$ and could be assigned to fully allowed $\pi\rightarrow\pi^*$ transitions, while the shoulder observed in MeCN has lower ε values ($0.5-0.7\times 10^4\ \text{M}^{-1}\,\text{cm}^{-1}$) and may be attributed to a partially forbidden transition of the same nature.

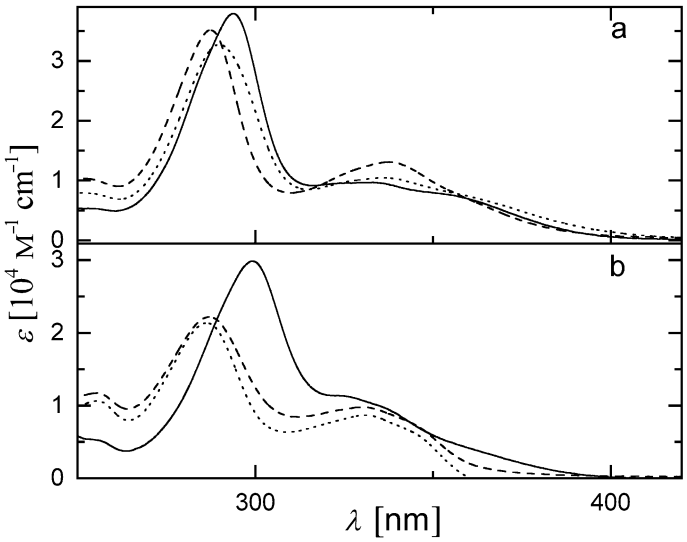

Fig. 1. *Absorption spectra of* a) *MOX and* b) *LVX in MeCN* (full line), *H_2O* (dashed line), *and PBS* (dotted line)

The fluorescence spectra of MOX and LVX show a broad band whose maximum depends on the solvent (*Fig. 2*). For both compounds, in MeCN, the emission maxima were at 500 nm, while, in aqueous solutions, they were blue-shifted by *ca.* 20–30 nm. In *Table 1*, the fluorescence properties of MOX and LVX in different solvents are reported. The deactivation path of the lowest singlet excited state (S_1) is strongly affected by the solvent as indicated by the values of the fluorescence quantum yields (ϕ_F). In particular, in aqueous media the radiative pathway is an efficient deactivation channel for S_1 since ϕ_F values of *ca.* 0.3 and 0.2 were measured for LVX and MOX, respectively. In the case of LVX, ϕ_F showed a dependency on the pH since a higher ϕ_F

value was measured in PBS, at higher pH, with respect to H_2O. On the other hand, in MeCN the fluorescence efficiency was much lower, especially for LVX, indicating that, in non-protic media, the radiative path is negligible.

The marked increase of ϕ_F values on going from MeCN to aqueous medium is likely to be related to the interactions of the protic solvent with the lone pair of the O-atom that, in general, causes an increase of the relative energy of the n, π^* singlet state with respect to that of the π,π^* state. If the two lowest singlet states of different nature, $^1(n,\pi^*)$ and $^1(\pi,\pi^*)$ are very close each other, an increase of the n,π^* energy causes an increase in the energy gap and a decrease in the vibronic interaction between them. The magnitude of the energy gap controls the value of the IC rate constant (proximity effect) as was discussed in detail by *Lai et al.* [13]. When the two states are close each

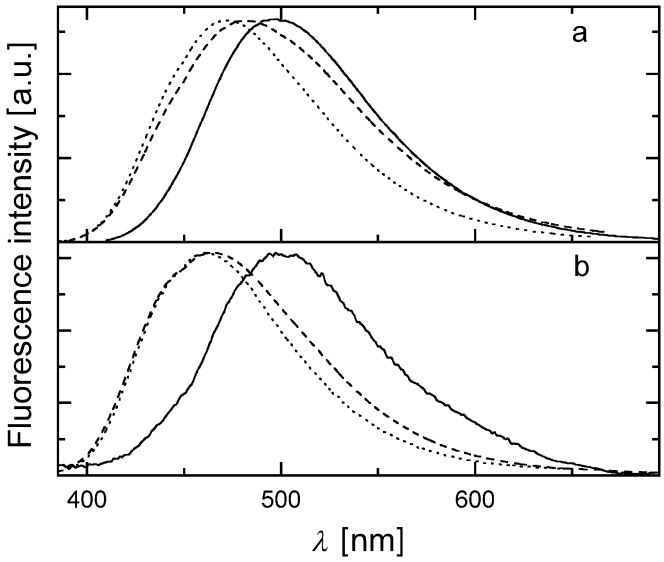

Fig. 2. *Normalized fluorescence spectra of* a) *MOX and* b) *LVX in MeCN* (full line), *H_2O* (dashed line), *and PBS* (dotted line)

Table 1. *Fluorescence Properties of* LVX *and* MOX *in MeCN, H_2O, and PBS Solutions*

Compound	Solvent	λ_{max} [nm]	ϕ_F	τ_F [%] [ns]	k_q (DNA) [$M^{-1}s^{-1}$]
LVX	PBS	462	0.35	6.2	
	ETN				2.2×10^{10}
	H_2O	465	0.25	6.9	
	MeCN	500	5×10^{-4}		
MOX	PBS	472	0.21	3.2 [89] 0.14	
	ETN				2.0×10^{10}
	H_2O	482	0.19	5.4 [93] 0.30	
	MeCN	497	4×10^{-2}		

other, the vibronic interaction is large and the singlet decays mainly through the internal conversion (quinolones in acetonitrile, ϕ_F negligible). When the energy gap increases, the rate constant of IC decreases, and competing processes take place (quinolones in aqueous medium, high ϕ_F values).

With the phase method shift, the fluorescence lifetimes of the quinolones under investigation were measured in aqueous media where the emission intensity was high enough to be detected with the set-up employed (*Table 1*). In the case of LVX, the frequency response curves were satisfactorily fitted by a mono-exponential function, and lifetimes of 6.2 and 6.9 ns were obtained in PBS and H_2O, respectively. For MOX, the phase and de-modulation *vs.* frequency curves could be fitted by bi-exponential function both in H_2O and PBS. The decay parameters were affected by the pH values since both the lifetimes of the short- and long-lived component were shorter in PBS although the relative weight was almost constant. For the long-lived component, lifetimes of 3.2 and 5.4 ns, and, for the short lived component, 0.14 and 0.34 ns were obtained in PBS and H_2O, respectively.

Laser flash photolysis experiments were carried out on both compounds under investigation in PBS and ETN buffers; the transient spectra recorded in PBS are shown in *Fig. 3*, similar results were obtained for the compounds in ETN. Upon direct excitation of MOX, the spectrum recorded at the end of the laser pulse presented two absorption bands with maxima at 390 and 720 nm. The kinetic analysis of the signals revealed that the bands decayed both with a first-order kinetics and with the same lifetime value of 0.08 μs, and it was not affected by the presence of molecular oxygen.

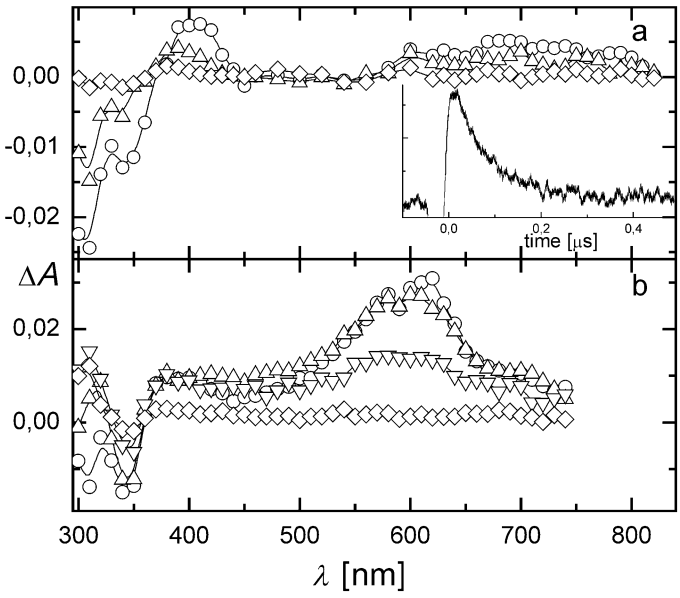

Fig. 3. *Time-resolved absorption spectra of* a) *MOX in PBS buffer, recorded 0.08* (○), *0.13* (△) *and 1.6* (◇) μs *after the laser pulse*; inset: *decay kinetics, recorded at 390 nm*; b) *LVX in PBS buffer, recorded 0.2* (○), *0.6* (△), *2.4* (▽), *and 8.0* (◇) μs *after the laser pulse* (λ_{exc} 308 nm)

This transient signal recorded for MOX in buffer solutions was attributed to the radical cation of the drug; in fact, it was sensitized, in MeCN, by chloranil (CHL), a well-known electron acceptor in the triplet state. In a typical experiment, the irradiation of CHL at 355 nm in the presence of MOX produced $CHL^{\bullet -}$ ($\lambda_{max} = 450$ nm), and the transient at 380 and 720 nm, attributed to $MOX^{\bullet +}$, formed during a timeframe corresponding to the rate of CHL triplet decay. Knowing the molar absorption coefficient of $CHL^{\bullet -}$ ($\varepsilon_{450} = 9700\ M^{-1}\ cm^{-1}$) [14], the absorption coefficient of $MOX^{\bullet +}$ could be determined. The absorption coefficient of $MOX^{\bullet +}$ at 720 nm was *ca.* $1000\ M^{-1}\ cm^{-1}$. Assuming that this parameter is not affected by the solvent and considering the product $\phi_{Tr} \times \varepsilon_{Tr}$ (*Table 2*) obtained in ETN, it was possible to estimate a quantum efficiency of 0.4 for the photoionization process of MOX. In aqueous media, the formation of the MOX radical cation ($MOX^{\bullet +}$) occurred during the laser pulse, probably due to the photoionization in the singlet and/or triplet state, although the absorption of the corresponding solvated electron was not clearly observed, likely due to the overlap with the absorption of MOX transient.

Table 2. *Properties of the Transients of* LVX *and* MOX *Produced by Directed Irradiation in PBS* ($\lambda_{exc} = 355$ nm)

Compound	λ_{max} [nm]	τ_{Tr} [μs]	$\phi_{Tr} \times \varepsilon$ [$M^{-1}\ cm^{-1}$]	k_q^{ox} [$M^{-1}\ s^{-1}$]
LVX	600	2.6	2650	1.8×10^9
MOX	390, *720*	0.08	400	$< 1.0 \times 10^5$

To gain deeper information on the nature of the transient species, flash photolysis experiments were carried out by exciting 3,3′-disulfonatobenzophenone (triplet energy donor) in the presence of MOX. Under our experimental conditions, the only transient observed was the triplet of 3,3′-disulfonatobenzophenone with a lifetime quenched to 100 ns. No further transients were detected. This result is in agreement with a triplet MOX with a short lifetime (≤ 100 ns), which likely prevents its detection even under direct excitation.

Laser excitation of LVX in PBS produced the transient spectra shown in *Fig. 3*, *b*. In this case, the transient signal showed a maximum at 610 nm, with a decay time of 2.6 μs. This transient was attributed to the lowest triplet state since it was produced within the laser pulse; it decayed according to first-order kinetics; it was quenched by molecular oxygen with a diffusion-controlled rate constant ($1.8 \times 10^9\ M^{-1}\ s^{-1}$); in toluene, it sensitized the triplet state of β-carotene ($\lambda_{max} = 540$ nm), a well-known triplet energy acceptor [15]. Unfortunately, the absorption intensity of the T-T band produced by irradiation of LVX was quite low in organic solvents (signal to noise ratio *ca.* 2), and this did not allow the measurement of the absorption coefficient (which probably was quite low), and consequently the triplet quantum yield could not be determined. The radical cation of LVX ($LVX^{\bullet +}$) was clearly observed only when it was sensitized by use of CHL in MeCN and was characterized in terms of absorption spectrum ($\lambda_{max} = 640$ nm) and absorption coefficient ($\varepsilon_{640} = 650\ M^{-1}\ cm^{-1}$). Upon excitation of LVX, the signal due to its radical cation was not detected likely because it is hidden by the triplet absorption, considering the spectral overlap and the low ε value of $LVX^{\bullet +}$.

Interactions with DNA. The addition of DNA to the fluoroquinolone solutions in ETN buffer induced spectral changes as shown by the ground-state spectra of MOX

and LVX in *Fig. 4* recorded at increasing DNA concentrations. For both compounds, the absorption at the longer-wavelength maximum was reduced upon increasing the DNA concentration. These observations indicated that static interactions are occurring between the fluoroquinolones and the DNA, which lead to the formation of complexes with lower molar absorption coefficients compared to those of the free drugs. The spectral changes induced by DNA were particularly evident when the concentration of biomolecule was higher than 1×10^{-4} M, corresponding to a [drug]/[DNA] ratio of *ca.* 0.15 and 0.05 for MOX and LVX, respectively. Under these experimental conditions, the samples were irradiated in order to check the occurrence of any photochemical process. In particular, MOX and LVX were irradiated at 330 and 340 nm, respectively, in the presence of DNA, and the samples were spectrophotometrically analyzed. No spectral changes were observed, indicating that the photoreaction is not an efficient path under the experimental conditions used.

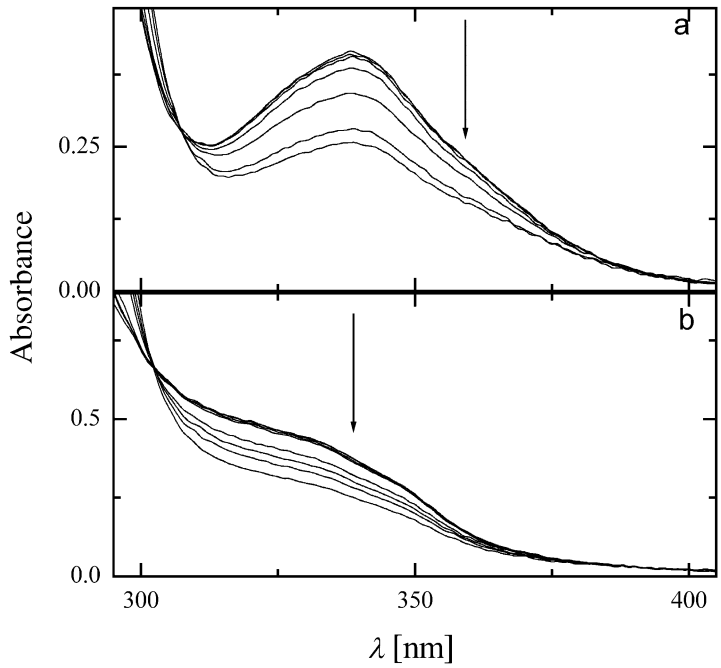

Fig. 4. *Absorption spectra of MOX* (*a*) *and LVX* (*b*) *in ETN buffer in the presence of increasing concentrations of DNA* ($0-1.5 \times 10^{-3}$ M)

The presence of DNA affected the decay channels of the lowest singlet excited state (S_1) of the quinolones under investigation. Steady-state fluorescence measurements in the presence of increasing concentrations of DNA revealed that the emission of MOX and LVX was quenched; in *Table 1*, the quenching rate constants (k_q) are reported. In both cases, the k_q values (*ca.* 2.0×10^{10} M^{-1} s^{-1}) are higher than the diffusional limits, indicating that static and dynamic interactions took place between the quinolones and DNA.

Laser flash photolysis experiments were carried out on the drug solutions in ETN buffer in the presence of DNA. The time-resolved spectra obtained in the presence of the biological substrate are reported in *Fig. 5*. For both systems, the transient spectrum recorded at early times, just at the end of the laser pulse, is identical to that obtained exciting the drugs alone.

In the case of MOX, the radical cation was not quenched by DNA under the experimental conditions used, and the signal decayed without significant spectral changes.

The addition of DNA to the LVX solution did not lead to the triplet quenching. However, the time evolution of the signals revealed the occurrence of spectral changes due to the formation of new transient species with absorption maxima at 420 and 570 nm. These bands can be tentatively assigned to the triplet state of the drug complexed with the biomolecule.

Photohemolysis. Cell membrane photodamage was investigated by using albino mouse erythrocytes as model system [16]. The hemolysis was followed by measuring the decrease in absorbance at 650 nm, which is proportional to the number of intact cells [17], and the results are reported in *Fig. 6*. All drugs were used at the concentration of 100 μM; for such a dose without irradiation, no significant hemolysis has been observed. The fluoroquinolones investigated, LVX and MOX, and ofloxacin (OFX) used as reference compound, are very photohemolytic, and under anaerobic

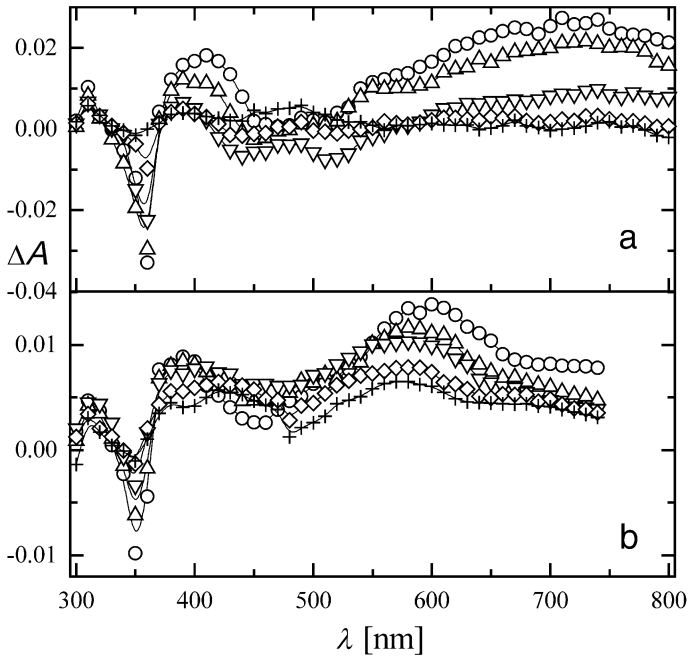

Fig. 5. *Time-resolved absorption spectra of* a) *MOX in ETN buffer in the presence of DNA, recorded 0.06* (○), *0.08* (△), *0.18* (▽), *0.40* (◇), *and 1.0* (+) μs *after the laser pulse*; b) *LVX in ETN buffer in the presence of DNA, recorded 0.22* (○), *0.46* (△), *2.5* (▽), *3.5* (◇), *and 6.4* (+) μs *after the laser pulse* (λ_{exc} 355 nm)

conditions they exhibit no significant difference, indicating that ROS (*i.e.*, singlet oxygen) are not involved in the photohemolytic process. It is interesting to note that the three fluoroquinolones have similar photohemolytic potencies, despite their different structures. Similar observations have been recently reported by *Yamamoto et al.* [18], who have demonstrated that the phototoxic potencies of fluoroquinolones might not be predictable by the photohemolysis studies. With the purpose to verify whether the photoproducts formed during the irradiation could be responsible or contribute to the observed photohemolysis, irradiated solutions of the three drugs were added to the RBC suspension. The experiments were monitored for 2 h, during which the RBC maintained their structure integrity (data not shown), indicating that the photoproducts are not involved in the photohemolytic effect.

Phototoxicity on 3T3 Cells. The *in vitro* cytotoxicity was evaluated by using a fibroblast cell line, a widely accepted *in vitro* model for skin irritation and photosensitization. All drugs at the indicated concentrations and without irradiation did not show cytotoxic effects. The results are presented in *Fig. 7.* As it can be seen, the decrease in cell viability was drug-concentration- and UVA-dose-dependent. OFX was the most phototoxic, and MOX was the least phototoxic compound. Also by this model, pre-irradiated solutions of the fluoroquinolones were tested to evaluate the cytotoxicity of photoproducts; the results obtained show that photoproducts are not cytotoxic (data not shown), indicating that the phototoxicity observed is mainly related to excited species and/or reactive oxygen species.

In an attempt to evaluate the possible mechanism(s) of the phototoxicity of these derivatives, a series of experiments were performed, in which various scavengers were included in the cell cultures during irradiation. The results of these studies are presented in *Table 3*.

Table 3. *Effects of Various Scavenging Agents on the Phototoxicity Induced by Fluoroquinolones in 3T3 Fibroblast Cells* (cell viability [%]). Cells were irradiated with a UVA dose of 8 J cm^{-2} in the presence of fluoroquinolones and various scavengers. Data are mean ± S.E.M. for four independent experiments.

	OFX	LVX	MOX
Drug alone	3.2 ± 0.05	20.9 ± 7.9	72.6 ± 3.9
SOD	43.7 ± 3.5[a])	45.7 ± 0.3[a])	64.8 ± 1.6
CAT	49.6 ± 3.6[a])	51.2 ± 3.5[a])	60.7 ± 5.1
BHA	37.3 ± 3.0[a])	60.3 ± 7.4[a])	80.2 ± 1.8
GSH	64.7 ± 0.6[a])	65.2 ± 4.5[a])	77.8 ± 1.2
MAN	59.1 ± 0.5[a])	68.3 ± 4.4[a])	76.4 ± 4.0
DMTU	43.4 ± 3.1[a])	61.3 ± 7.4[a])	79.5 ± 0.3

[a]) $p < 0.01$ *vs.* Drug alone

The scavengers used were SOD (2000 UI/ml) and catalase (2000 UI/ml), which scavenge $O_2^{-\bullet}$ and H_2O_2, respectively, BHA (10 μM) and GSH (1 mM), two radical scavengers, and DMTU (1 mM) and MAN (10 mM), which scavenge hydroxyl radicals ($OH^{\bullet}$).

Scavengers alone did not have any effect on cell viability during UVA exposure (data not shown). Significant protection from LVX- and OFX-induced phototoxicity

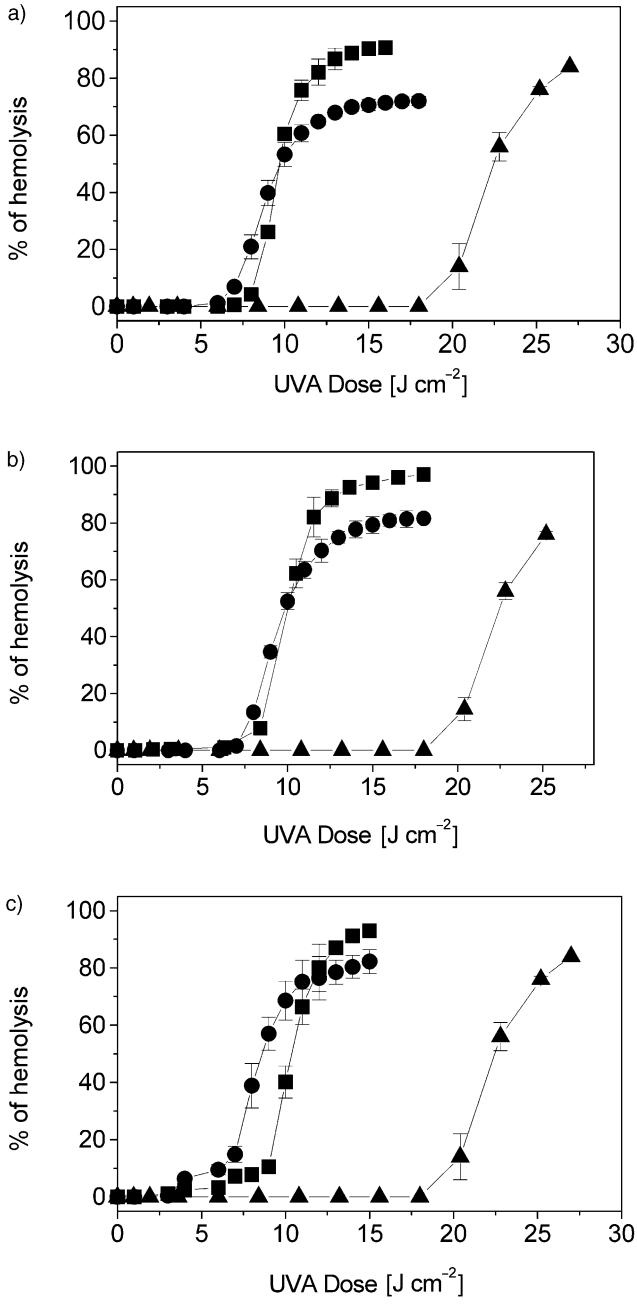

Fig. 6. *Percentage of hemolysis of mouse red blood cells photoinduced by* a) *LVX*, b) *OFX*, *and* c) *MOX examined at the concentration of 100* μM *in the presence* (●) *and in the absence* (■) *of oxygen and* ▲ *represents the test in the absence of drug*

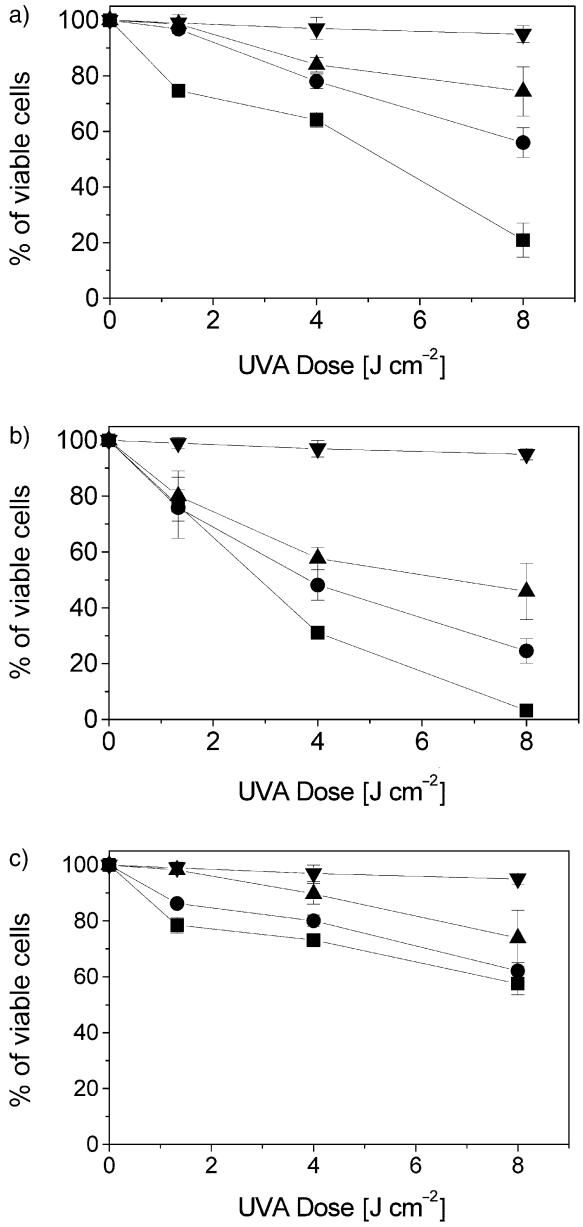

Fig. 7. *Effect of fluoroquinolone photosensitization of* a) *LVX*, b) *OFX*, *and* c) *MOX on 3T3 fibroblasts.* The cells were treated with the drugs at different concentrations: 100 μM (■), 50 μM (●), 25 μM (▲), no drug (▼) and various doses of UVA. The viability was measured with the MTT method as described in *Exper. Part*. Points are mean ± S.E.M. for three independent experiments performed in quadruplicate.

was observed with SOD and CAT. Furthermore, the addition of two free radical scavengers, BHA and GSH, and the $OH^{\bullet}$ scavengers, MAN and DMTU, also demonstrated a significant protective effect on fluoroquinolone-induced phototoxicity. In contrast, no effects were observed with MOX, probably due to its low inherent phototoxicity. These data indicate that LVX and OFX are able to induce cytotoxicity through the formation of superoxide anion.

Mitochondrial Damage. To investigate which cellular sites are involved in the phototoxicity induced by fluoroquinolones, we focused our attention on mitochondria. It has been previously shown that mitochondrial alterations are involved in cell death caused by many photosensitizers including fluoroquinolones [19].

As recently demonstrated [19], lysosomes are major sites of localization of fluoroquinolones although other subcellular organelles can also be the target of fluoroquinolones. In fact, we also found that, upon fluoroquinolone addition, fluorescence in 3T3 cells was partially localized in mitochondria (data not shown), and co-localized with that of TMRM, a lipophilic cation commonly used for the assessment of the mitochondrial potential ($\Delta\psi_m$) [20][21]. Thus, we have investigated whether mitochondrial dysfunction is associated with fluoroquinolone-induced phototoxicity. The experiments performed to assess the changes in mitochondrial functions are shown in *Fig. 8*. The $\Delta\psi_m$ was monitored by means of TMRM fluorescence. To exclude artifacts due to the different loading capacity of the various cells, which can be erroneously interpreted as $\Delta\psi_m$ differences, after each treatment the cells were treated with FCCP, an uncoupler of oxidative phosphorylation, which abolishes $\Delta\psi_m$. Thus, in each cell, the difference of fluorescence intensities obtained before and after FCCP provides a reliable assessment of $\Delta\psi_m$. It can be seen from *Fig. 8* that the decline of $\Delta\psi_m$ is detectable with OFX, used at the concentration of 50 μM, and LVX at 6 h after the irradiation reaching a maximum after 24 h. On the contrary, the $\Delta\psi_m$ of the cells irradiated in the presence of MOX remain at the level of irradiated control.

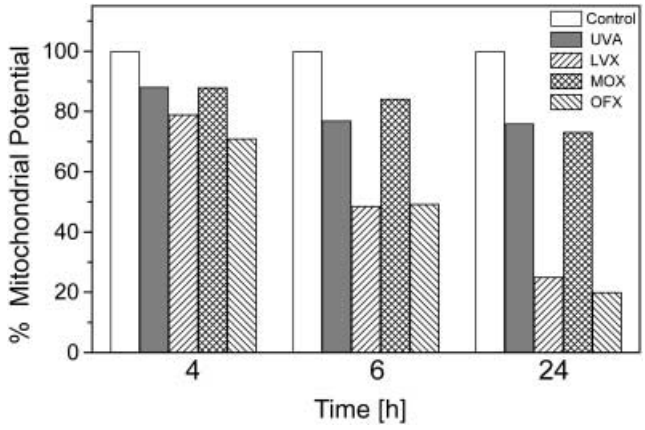

Fig. 8. *Decrease of the mitochondrial potential* ($\Delta\psi_m$) *in 3T3 cells after irradiation* (8 J cm^{-2}) *in the presence of the fluoroquinolones at the concentration of 100* μM *for LVX and MOX, and 50* μM *for OFX*

Lipid Peroxidation. Peroxidation of erythrocyte membrane unsaturated lipids during UVA irradiation was determined by assaying TBARS formed as secondary products of lipid peroxidation [22].

Fig. 9 (*Top*) shows the results on erythrocyte membrane lipid peroxidation induced by the three drugs exposed to UVA irradiation for various times. The photoperoxidation induced by OFX and LVX increased sharply with the irradiation time. On the contrary, MOX shows a peroxidation level similar to that of the irradiated control. The photoinduced lipid peroxidation has been examined also in the presence of scavengers, and the results are presented in *Fig. 9* (*Bottom*). It can be noted that SOD, CAT, BHA, and DMTU exert a significant protective effect on fluoroquinolone-induced lipid peroxidation, in good agreement with the data on 3T3 cells reported above.

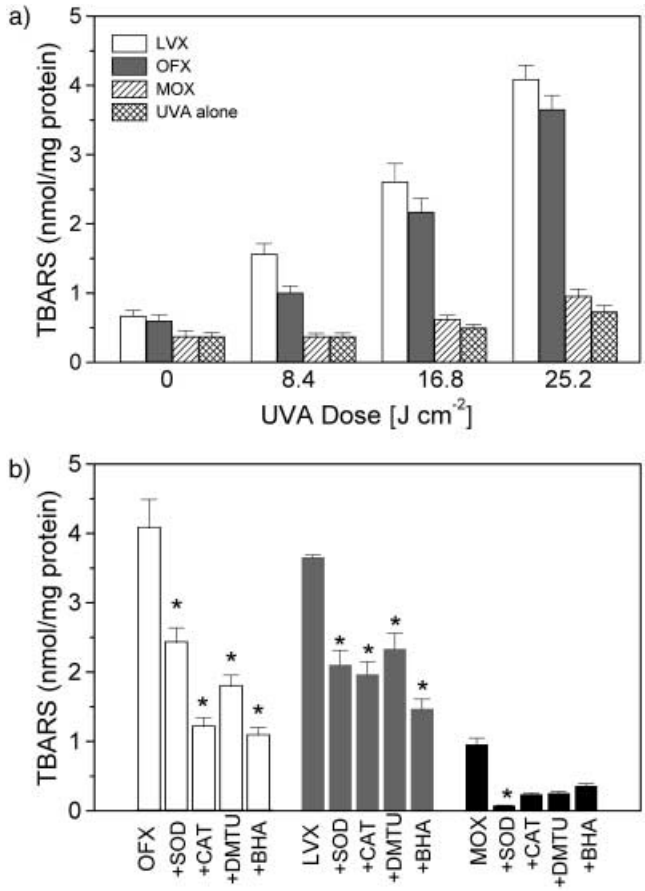

Fig. 9. Top: *Formation of thiobarbituric acid reactive substances (TBARS) in human red blood cell membranes (ghost), following irradiation in the presence of the fluoroquinolone derivatives at a concentration of 100 μM.* Points are means ± S.E.M. Bottom: *Effect of different scavengers on lipid peroxidation of erythrocyte ghosts by the fluroquinolones irradiated at a UVA dose of 24 J cm^{-2}.* * $p < 0.01$ *vs.* Drug alone.

Protein Photodamage. The photosensitization ability of the drugs towards other components of cellular membranes, such as proteins, was estimated by measuring the photoinduced cross-linking in erythrocyte ghost proteins [23]. Light-induced cross-linking of spectrin, a protein associated with the cytoplasmic side of the RBC membrane, in the presence of compounds was detected by the partial or total disappearance of the two spectrin bands (220000 and 245000 D) on SDS-PAGE gel: cross-linked aggregates cannot run inside the gel and remain at the top.

Fig. 10 shows the effect of the treatment of erythrocyte membrane with the three compounds. As observed, increasing irradiation times led to a gradual disappearance of the two spectral bands, whereas there is the concomitant appearance of a protein photoaggregate at the top of the gel. The densitometric analysis (data not shown) reveal that OFX is the most active compound followed by LVX and MOX, in good agreement with the phototoxicity order observed in the 3T3 cells. Interestingly, a significant reduction of the photodegradation of the spectrin is observed under anaerobic conditions for all three drugs.

DNA Photodamage. Most of the fluoroquinolones used today in therapy have demonstrated a high degree of DNA photodamage, and this can account for their capability of enhancing UVA-induced phototumorigenesis [24–27].

To determine whether LVX and MOX were able to photosensitize DNA-strand-break activity, they were evaluated by using supercoiled circular DNA because it is a very sensitive tool for damage detection [25]. In addition to frank strand break, we have also evaluated whether purine and/or pyrimidine bases were involved in the oxidative damage to DNA by using base-excision-repair enzymes Fpg an Endo III, respectively.

Supercoiled circular DNA allows the detection of structural alterations such as strand breaks or damaged bases. DNA Strand break can be induced either directly (frank strand breaks) or indirectly by using DNA-repair enzymes; in this case, we determined the number of DNA modifications sensitive to the following repair enzymes: *i*) Fpg protein, which has been demonstrated to recognize 8-hydroxyguanine, purines whose imidazole ring is open (Fapy residues), and sites of base loss (apurinic sites); *ii*) endonuclease III, which is known to recognize, in addition to apurinic sites, 5,6-dihydropyrimidines derivatives. Damaged base release is followed by a β-δ reaction and a β-elimination step, respectively, resulting in DNA breakage [28].

In addition to endonuclease-sensitive modifications, the number of single-strand breaks generated by the excited photosensitizers were quantified. *Fig. 11* shows the results obtained for the three fluoroquinolones tested at a [drug]/[DNA] ratio of 0.8. As it can be noted for all compounds, the formation of a single-strand break, expressed as the percentage of form II, is low and becomes significantly different from the irradiated control only at the highest UVA dose employed (30 J cm^{-2}). On the contrary, high level of single-strand breaks can be detected after enzyme digestion for OFX and LVX, clearly indicating that both purine and pyrimidine bases were oxidized, whereas only a slight increase was observed for MOX.

Conclusions. – The phototoxicity mechanism for MOX and LVX seems particularly complex because the photobiological tests *in vitro* show the involvement of free

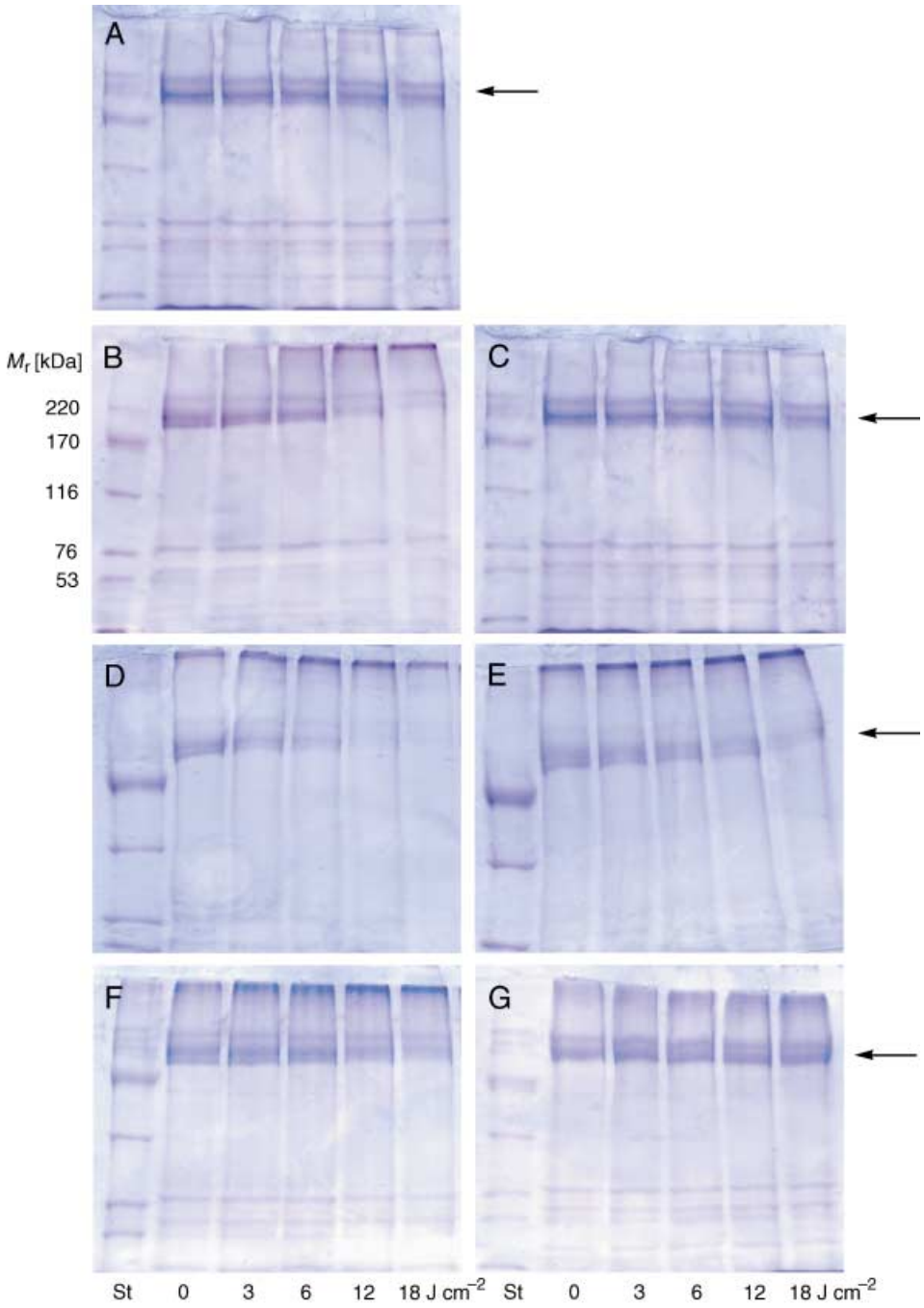

Fig. 10. *Electrophoretic pattern of the photoinduced cross-linking of spectrin in RBC ghosts irradiated at the indicated doses in the presence of fluoroquinolones at the concentration of 100* μM *of LVX, OFX, and MOX in the presence of oxygen* (panels *B*, *D*, and *F*, resp.), *and in the absence* (panels *C*, *E*, and *G*, resp.). Panel *A* represents the test in absence of drugs. The spectrin band is indicated by an arrow. St is a mixture of molecular-weight standards, of which the values are depicted in the left of the figure.

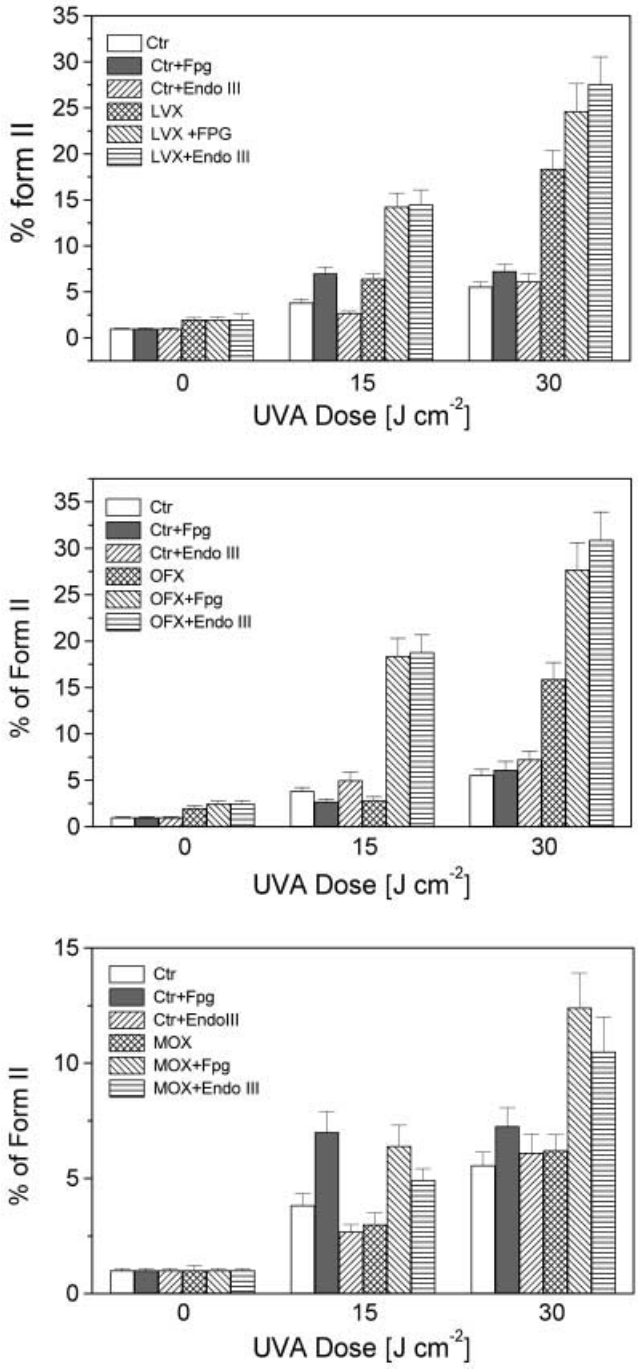

Fig. 11. *DNA-Strand breaks photoinduced by the fluoroquinolones expressed as percentage of form II obtained after densitometric analysis of the gel*. pBR322 supercoiled circular DNA was irradiated at the indicated doses and then treated as described in the *Exper. Part*.

radicals and ROS species, as well as a decrease of the of the phototoxic effects in the absence of oxygen.

MOX, which is an 8-MeO-substituted fluoroquinolone, showed a lower phototoxicity in all of the employed tests; this observation could be related to its photostability [29] and confirms previous data, according to which the introduction of an 8-MeO moiety in the quinolone ring significantly reduces the phototoxicity of fluoroquinolones [30][31]. In this context, the photophysical and flash photolytic experiments can provide evidence on the involved phototoxic species and on their production. MOX showed a high quantum yield of photoionization (0.4) with production of the cation radical $MOX^{\bullet+}$, but it does not present high phototoxicity. This means that all charged species produced in the photoionization process are scarcely reactive with biological targets either, because there is fast recombination (in fact, $MOX^{\bullet+}$ has a lifetime of 80 ns) or because the intrinsic reactivity of the charged species formed is low. Also the phototoxicity attributable to the singlet oxygen that can be produced by the short-lived triplet of MOX should be low.

The cytotoxicity of LVX is enhanced after UVA irradiation, although to a lesser degree in comparison with the racemic mixture OFX used in this study as a reference compound. Laser excitation of LVX shows the formation of the triplet state that can give singlet oxygen (mechanism *Type-II* or other *Type-I* photoprocesses). Both LVX and OFX produce phototoxic reactive species towards the biological targets. However, photoprocesses taking place in the singlet state (*Type-I* mechanism) cannot be excluded for these drugs, particularly with DNA, where there is interaction in the ground state. The use of suitable scavengers indicates the formation of radical species under UVA irradiation. Indeed, cytotoxicity and lipid peroxidation are markedly inhibited by two typical free-radical scavengers BHA and GSH. Furthermore, the addition of MAN and DMTU also demonstrated a significant protective effect on fluoroquinolone-induced phototoxicity. These findings strongly suggest that $OH^{\bullet}$ generation plays a role in the phototoxicity induced by this fluoroquinolones. Interestingly, the observation that the exogenously added enzymes CAT and SOD, which do not enter the cells, are protective against the phototoxic effects of the LVX indicates that the ROS responsible for the effect act at the membrane level. In this context, the membrane damage monitored by lipid peroxidation and protein cross-link seems to confirm this hypothesis. These data are in good agreement with the data reported by *Wagai* and *Tawara* [6][7], who have demonstrated that the phototoxicity associated with quinolones in balb/c mice was initiated by the generation of ROS in the target tissue, which specifically involved hydroxyl radical, as well superoxide anion and hydrogen peroxide. Moreover, it has also been reported that the initial steps in the quinolone phototoxicity probably involve hydroxyl-radical attack on the cell membrane and mitochondria [32]. In this context, we have demonstrated a gradual loss of the mitochondrial potential ($\Delta\psi_m$) for LVX and OFX, suggesting that the mitochondria are readily damaged by photosensitization with these fluoroquinolones. Whether these mitochondrial alterations are critical events in the cell death deserves further study.

Experimental Part

General. MOX and LVX were extracted from commercial tablets. Their purity, confirmed by HPLC analysis, was over 99%. OFX Hydrochloride was purchased from *Sigma Chemical Company* (St. Louis, MO, USA). TBA, DMTU, SOD, CAT, BSA, 1,1,3,3-tetraethoxypropane, MTT, agarose, BHA, salmon testes DNA, and GSH were also obtained from *Sigma Chemical Company* (St. Louis, MO, USA). Acrilamide and *N,N′*-methylene[bisacrylamide], ammonium persulfate, TEMED (= *N,N,N′,N′*-tetramethylethylenediamine), pBR322 DNA, and ethidium bromide soln. were purchased from *Amersham Biosciences. Coomassie Brilliant Blue G-250* was purchased from *BioRad Laboratories* (Segrate, I-Milano). TMRM was purchased by *Molecular Probes* (Eugene, OR, USA). The two base-excision repair enzymes (BER), formamido-pyrimidine glycosilase (FPG) and endonuclease III, were a generous gift from Dr. *S. Boiteux* (CEA, F-Fontenay aux Roses).

Photophysical Measurements. Benzophenone (*Aldrich*; gold label) was used as received; disodium 3,3′-disulfonatobenzophenone was that used in a previous work [33]. MeCN (*Fluka*; spectro-grade) distilled water (pH 5.5), PBS (= phosphate-buffered saline; 0.01M phosphate buffer, 0.135M NaCl, pH 7.2), and ETN buffer, (10 mM *Tris* · HCl, 1 mM ethylenediaminetetraacetic acid (EDTA), 10 mM NaCl, pH 7.2).

Absorption spectra of the sample solns. were recorded with a *Perkin-Elmer* spectrophotometer (*Lambda 800*). Fluorescence spectra, corrected for the instrumental response, and quantum yields were measured with a *Spex* (*Fluorolog F112AI*) spectrophotofluorometer in aerated soln. (absorbance < 0.25 at λ_{exc}) with anthracene in de-aerated EtOH ($\phi_F = 0.27$) [34] as standard.

The fluorescence lifetimes, τ_F (mean deviation of three independent experiments, *ca.* 5%), were measured with a *Spex Fluorolog-τ2* system, by using the phase-modulation technique (excitation wavelength modulated in the 1–300-MHz range; time resolution *ca.* 20 ps). The frequency-domain intensity decays (phase angle and modulation *vs.* frequency) were analyzed with the *Global Unlimited*™ (rev.3) global analysis software [35].

Laser flash photolysis experiments were carried out with the previously described set-up [36][37] based on a Nd:YAG Continuum laser (*Surelite II*, third harmonics, $\lambda_{exc} = 355$ nm, pulse width *ca.* 7 ns, and energy ≤ 1 mJ pulse^{-1}) and a XeCl excimer *Lambda Physik* laser (*EMG 50E*, $\lambda_{exc} = 308$ nm, pulse width *ca.* 20 ns, and energy ≤ 1 mJ pulse^{-1}). The transient spectra were obtained by monitoring the optical-density change at intervals of 5–10 nm over the 300–800-nm range and by averaging at least ten decays at each wavelength. The transient lifetimes were measured at an absorbance of *ca.* 0.2; the concentration effect on triplet lifetime was not investigated. First-order kinetics was observed for the decay of the lowest triplet state (T-T annihilation was prevented by the low excitation energy). The $\Delta\varepsilon_{Tr} \times \phi_{Tr}$ product (where $\Delta\varepsilon_{Tr}$ is the difference between the molar absorption coefficients of the transient and the ground-state at the observation wavelength, and ϕ_{Tr} is the quantum yield for the transient formation) was measured at the absorption maxima of the transients. The calibration of the experimental setup was made with an optically matched soln. of benzophenone in MeCN ($\phi_T = 1$ and $\Delta\varepsilon_T = 6500$ M^{-1} cm^{-1}) [38]. When the transient was the lowest triplet state of quinolones, $\Delta\varepsilon_T$ (and then ϕ_T values) was determined by the energy-transfer method by using disodium 3,3′-disulfonatobenzophenone as a donor, assuming for it the same triplet characteristics of benzophenone [39]. All measurements were carried out at $22 \pm 2°$; the solns. were saturated by bubbling with Ar. The experimental errors on τ_T values were estimated to be *ca.* ±10% while those on $\Delta\varepsilon_T$ and ϕ_T were ±15%.

Irradiation Procedure. One or two *HPW 125 Philips* lamps, mainly emitting at 365 nm, were used for irradiation experiments. The total energy was detected with a *Cole-Parmer Instrument Company* radiometer (Niles, IL) equipped with a *365-CX* sensor.

Photohemolysis. Whole blood, collected from untreated albino mouse with heparin as anticoagulant, was washed with PBS, centrifuged, and the supernatant and the buffy coat were discarded. The procedure was repeated until the supernatant was colorless. RBC were resuspended in PBS (1:1000) and used within 48 h. For the photohemolysis experiments, RBC were incubated for 15 min at 37° in the dark in the presence of the compounds, dissolved in DMSO. The suspension was then irradiated with increasing UVA doses under gentle shaking in a controlled-temp. bath. Analogous experiments were performed in N_2-purged samples by gently bubbling N_2. Hemolysis was determined by spectrophotometric measurements at 650 nm where intact cells absorb [16].

Cell Cultures. Balb/c mouse 3T3 fibroblasts were grown in DMEM medium (*Dulbecco*'s modified *Eagle* medium, *Sigma Co.*) supplemented with 115 units/ml of penicillin G (*Life Technologies*, I-Milano), 115 μg/ml streptomycin (*Life Technologies*, I-Milano), and 10% fetal calf serum (*Life Technologies*, I-Milano). Individual wells of 96-well tissue culture microtiter plate (IWAKI Japan) were inoculated with 100 μl of DMEM containing 5×10^3 mouse 3T3 cells. The plate was incubated at 37° in a humidified 5% incubator for 72 h to form a monolayer of *ca.* 80% confluence.

After the medium was removed, 100 µl of the drug soln., dissolved in DMSO and diluted with *Hank*'s Balanced Salt Solution (HBSS pH 7.2), was added to each well. When scavengers were used, they were dissolved in HBSS, mixed with quinolone solns., and placed in a well. The plate was then incubated for 30 min in an atmosphere of 5% CO_2 at 37°, and then irradiated. After irradiation, the soln. was replaced by the medium, and the plates were incubated for 24 h. Cell viability was assayed by the MTT test as described in [40][41].

Fluorescence Microscopy and Mitochondrial Potential. At different times after UVA treatment, 3T3 cells were washed with HBSS and then incubated for 15 min at 37° with 25 nM of TMRM. Cyclosporin H (1.6M) was also added to inhibit multidrug-resistance pumps, which can affect TMRM loading [21]. Cellular fluorescence images were acquired with an *Olympus IMT-2* inverted microscope, as described in [20]. For detection of TMRM fluorescence, 568 ± 25-nm excitation and 585-nm longpass emission filter settings were used. Data were acquired and analyzed with *Metamorph* software (*Universal Imaging*). Mitochondria were identified as region of interest (ROI), and at least 30 ROIs were considered for each experiments. The decrease in fluorescence intensities induced by FCCP was expressed as the difference of the values obtained before and after the addition of uncoupler. The values of these differences obtained in the treated cells were normalized to the difference values of the untreated cells (control).

Erythrocyte Ghost Preparation. Ghosts were prepared from heparinized human blood according to the gradual osmotic lysis method of *Steck* and *Kant* [42]. White membranes (ghosts) were resuspended in PBS buffer. Membrane protein contents were determined as described in [43], with BSA as a standard.

Lipid Peroxidation. Ghost were irradiated in 1.2-ml aliquots in 24 well plates in the presence of the fluoroquinolones. After irradiation, 1.0 ml was removed for the TBARS assay, which was conducted as described in [44]. A standard curve of 1,1,3,3-tetraethoxypropane was used to quantitate the amount of malonaldehyde produced. Data are expressed in terms of nanomoles of TBARS normalized to the membrane protein content.

Protein Photo-Cross-Link. To the membrane suspension (1.0 mg/ml protein concentration), the test compounds were added and irradiated. The membrane samples were reduced and denatured by addition of 2-sulfanylethanol and SDS at 90° for 3 min, and bromophenol blue (BPB) was added before polyacrylamide gel electrophoresis (SDS-PAGE) analysis (5% running gel, 3% stacking gel). The quantitation of the bands, stained with *Coomassie Brilliant Blue R-250* was achieved by image analyzer software *Quantity One* (*BioRad*, I-Milano).

pBR322 DNA Strand Breaks. Each pBR322 DNA sample (100 ng) dissolved in TE buffer (10 mM *Tris* · HCl, 1 mM EDTA, pH 7.5) was irradiated with increasing UVA doses in the presence of the compounds under examination. After irradiation, two aliquots of the sample were incubated at 37° with Fpg and Endo III (Endonuclease III), respectively, as described by *Pflaum et al.* [45]. The samples were loaded on 1% agarose gel, and the run was carried out in TAE buffer (0.04M *Tris*-acetate, 1 mM EDTA) at 50 V for 4 h. After staining in ethidium bromide soln., the gel was washed with H_2O, and the DNA bands were detected under UV radiation with a UV transilluminator. Photographs were taken with a digital photocamera *Kodak DC256* and the quantitation of the bands was achieved by image analyzer software *Quantity One* (*BioRad*, I-Milano). The fractions of supercoiled DNA (Form I) and open circular (Form II) were calculated as described in [46].

Statistics. When reported, average data are presented as the means ± standard error of the mean. Where appropriate, statistical comparisons were performed by analysis of the variance (ANOVA) and *Student*'s *t* test.

The authors are thankful for the financial support of the *Ministero per l'Università e la Ricerca Scientifica e Tecnologica* (Rome) in the framework of the *Programmi di Ricerca di Interesse Nazionale* (project: *Photoprocesses of Interest for Applications*).

REFERENCES

[1] V. T. Andriole, *Drugs* **1999**, *58,* Suppl. 2, 1.
[2] J. M. Domagala, *J. Antimicrob. Chemother.* **1994**, 22, 685.
[3] R. Stahlmann, H. Lode, in 'The Quinolones', Ed. V. T. Andriole, Academic Press, London, 1998, p. 369.
[4] D. C. Hooper, J. S. Wolfson, *Antimicrob. Agents Chemother.* **1985**, *28*, 716.
[5] G. Kleacak, F. Urbach, H. Urwyler, *J. Photochem. Photobiol., B* **1997**, *37*, 174.
[6] N. Wagai, K. Tawara, *Arch. Toxicol.* **1992**, *65*, 495.
[7] N. Wagai, K. Tawara, *Arch. Toxicol* **1992**, *66*, 392.
[8] N. Umezawa, K. Arakane, A. Ryu, S. Mashiko, M. Hirobe, T. Nagano, *Arch. Biochem. Biophys.* **1997**, *342*, 275.

[9] L. J. Martinez, R. H. Sik, C. F. Chignell, *Photochem. Photobiol.* **1998**, *67*, 399.
[10] M. Tanaka, M. Otsuki, T. Une, T. Nishino, *J. Antimicrob. Chemother.* **1990**, *26*, 659.
[11] T. Une, T. Fujimoto, K. Sato, Y. Osada, *Antimicrob. Agents Chemother.* **1988**, *32*, 1336.
[12] C. S. Lewin, S. G. Amyes, *J. Med. Microbiol.* **1989**, *30*, 227.
[13] T. I. Lai, B. T. Lim, E. C. Lim, *J. Am. Chem. Soc.* **1982**, *104*, 7631.
[14] J. J. André, G. Weil, *Mol. Phys.* **1968**, *15*, 97.
[15] C. V. Kumar, L. Qin, P. K. Das, *J. Chem. Soc., Faraday Trans.* **1984**, *80*, 783.
[16] D. G. Robertson, D. L. Bailey, R. A. Martin, *Photochem. Photobiol.* **1991**, *53*, 455.
[17] D. P. Valenzeno, J. W. Trank, *Photochem. Photobiol.* **1985**, *42*, 335.
[18] T. Yamamoto, Y. Tsurumaki, M. Takei, M. Hosaka, Y. Oomori, *Toxicol. in Vitro* **2001**, *15*, 721.
[19] G. Ouedraogo, P. Morliere, M. Bazin, R. Santus, B. Kratzer, M. A. Miranda, J. V. Castell, *Photochem. Photobiol.* **1999**, *70*, 123.
[20] V. Petronilli, G. Miotto, M. Canton, M. Brini, R. Colonna, P. Bernardi, F. Di Lisa, *Biophys. J.* **1999**, *76*, 725.
[21] P. Bernardi, L. Scorrano, R. Colonna, V. Petronilli, F. Di Lisa, *Eur. J. Biochem.* **1999**, *264*, 678.
[22] W. Girotti, *J. Lipid Res.* **1998**, 39, 1529.
[23] M. P. Merville, J. Piette, J. Decuypier, C. M. Calberg-Bacq, A. Van De Vorst, *Chem.-Biol. Interact.* **1983**, *44*, 275.
[24] L. J. Martinez, C. F. Chignell, *J. Photochem. Photobiol., B* **1998**, *45*, 51.
[25] L. Marrot, J. P. Belaidi, C. Chaubo, J. R. Meunier, P. Perez, C. Agapakis-Causse, *Toxicol. in Vitro*, **2001**, *15*, 131.
[26] H. J. Reavy, N. J. Traynor, N. K. Gibbs, *Photochem. Photobiol.* **1997**, *66*, 368.
[27] A. A. Chetalat, S. Albertini, E. Gocke, *Mutagenesis* **1996**, *11*, 497.
[28] C. J. Burrows, J. G. Muller, *Chem. Rev.* **1998**, *98*, 1109.
[29] T. E. Spratt, S. S. Schultz, D. E. Levy, D. Chen, G. Schlüter, G. M. Williams, *Chem. Res. Toxicol.* **1999**, *12*, 809.
[30] M. Matsumoto, K. KoJima, H. Nagano, S. Matsubara, T. Yokota, *Antimicrob. Agents Chemother.* **1992**, *36*, 1715.
[31] K. Marutani, M. Matsumoto, Y. Otabe, M. Nagamuta K. Tanaka, A. Miyoshi, T. Hasegawa, H. Nagano, S. Matsubara, R. Kamide, T. Yokota, F. Matsumoto, Y. Ueda, *Antimicrob. Agents Chemother.* **1993**, *37*, 2217.
[32] G. Ouedraogo, P. Morliere, R. Santus, M. A. Miranda, J. V. Castell, *J. Photochem. Photobiol., B* **2000**, *58*, 20.
[33] G. Favaro, A. Romani, *J. Chem. Soc. Faraday Trans.* **1993**, *89*, 699.
[34] D. F. Eaton, in ' Handbook of Organic Photochemistry', Vol. 1, Ed. J. C. Scaiano, CRC Press, Boca Raton, FL, 1989, p. 231, and refs cit. therein.
[35] J. M. Beechem, E. Gratton, M. Ameloot, J. R. Kutson L. Brand, 'Fluorescence Spectroscopy, Vol. 1, Principles and Techniques', Ed. J. R. Lakowicz, Plenum Press, New York, 1988 and refs. cit. therein.
[36] H. Görner, F. Elisei, G. G. Aloisi, *J. Chem. Soc., Faraday Trans.* **1992**, *88*, 29.
[37] A. Romani, F. Elisei, F. Masetti, G. Favaro *J. Chem. Soc., Faraday Trans.* **1992**, *88*, 2147.
[38] I. Carmichael, G. L. Hug, *J. Chem. Phys. Ref. Data* **1986**, *15*, 1.
[39] J. P. Fouassier, D. J. Lougnot, I. Zuchowics, P. N. Green H. J. Timpe, K. P. Kronfeld, U. Müller, *J. Photochem.* **1987**, *36*, 347.
[40] F. Elisei, G. Aloisi, L. Latterini, U. Mazzuccato, G. Viola, G. Miolo, D. Vedaldi, F. Dall'Acqua, *Photochem. Photobiol.* **2002**, *75*, 11.
[41] G. Miolo, G. Viola, D. Vedaldi, F. Dall'Acqua, A. Fravolini, O. Tabarrini, V. Cecchetti, *Toxicol. in Vitro* **2002**, *16*, 683.
[42] T. L. Steck, J. A. Kant, *Methods Enzymol.* **1974**, *31*, 172.
[43] G. L. Peterson, *Anal. Biochem.* **1977**, *83*, 346.
[44] J. A. Beuge, S. D. Aust, *Methods Enzymol.* **1978**, *30*, 302.
[45] M. Pflaum, S. Boiteux, B. Epe, *Carcinogenesis* **1994**, *15*, 297.
[46] T. A. Ciulla, J. R. van Camp, E. Rosenfeld, I. E. Kochevar, *Photochem. Photobiol.* **1989**, *49*, 293.

Received November 11, 2003